Numerical Simulation of Coextrusion from a Circular Die

E. MITSOULIS and F. L. HENG, *Department of Chemical Engineering, University of Ottawa, Ottawa, Ontario, Canada K1N 9B4*

Synopsis

A numerical simulation of coextrusion flow in a capillary die has been undertaken for polymer melts used in a previously reported experimental study of coextrusion. Viscosity data are used for PS, HDPE, and LDPE melts. A Newton–Raphson scheme is employed to solve the equations for a fully developed pressure-driven flow of two concentric layers in a capillary. A finite element method is used to simulate the full flow field behavior, including determination of the interface and free surface of the exiting stream. Double nodes have been used at the interface to ensure continuity of velocities and stresses and to capture the pressure discontinuities. Pressure gradients, extrudate swell, interface swell, and other relevent flow characteristics are presented and compared with the experimental findings. The finite element analysis revealed that satisfactory convergence of the interface location is found for the cases when the less viscous material wets the capillary walls, which is also the preferential configuration in coextrusion. For the opposite configuration, convergence proved either difficult or impossible depending upon the viscosity ratio. Discrepancies were found to exist between the theoretically predicted and experimentally measured pressure gradients.

INTRODUCTION

In recent years coextrusion is commonly practiced by the polymer processing industry for the production of multilayered films, fibers, pipes, wire coatings, etc. The coextrusion process consists of combining two or more different melt streams in a feedblock, as shown schematically in Figure 1. Studies of such flows have been carried out both experimentally and analytically.[1] The experimental studies indicate that complex interface shapes arise in the extrudate, especially when the melts are fed side-by-side. The encapsulation of the more viscous component by the less viscous one has been observed in both circular and rectangular geometries.[2-5] This phenomenon has been analyzed in terms of dissipated energy[6-9] but solution of the full flow equations along with prediction of this phenomenon has not been achieved yet.

The analytical studies so far deal basically with the fully developed Poiseuille flow of two or more fluids within the die[10,11] and its stability.[12] Experimental stability studies have also been done.[13-15] Numerical solutions of the flow equations have been given making use of the lubrication approximation (unidirectional flow).[16] Nonisothermal effects have also been included,[17-20] showing a rather small influence of the thermal phenomena on the variations of the interface location along the die.

Since in all practical situations the fluids to be coextruded meet at an angle and flow together hereafter, an unknown *a priori* interface is present and

Journal of Applied Polymer Science, Vol. 34, 1713–1725 (1987)
 CCC 0021-8995/87/041713-13$04.00

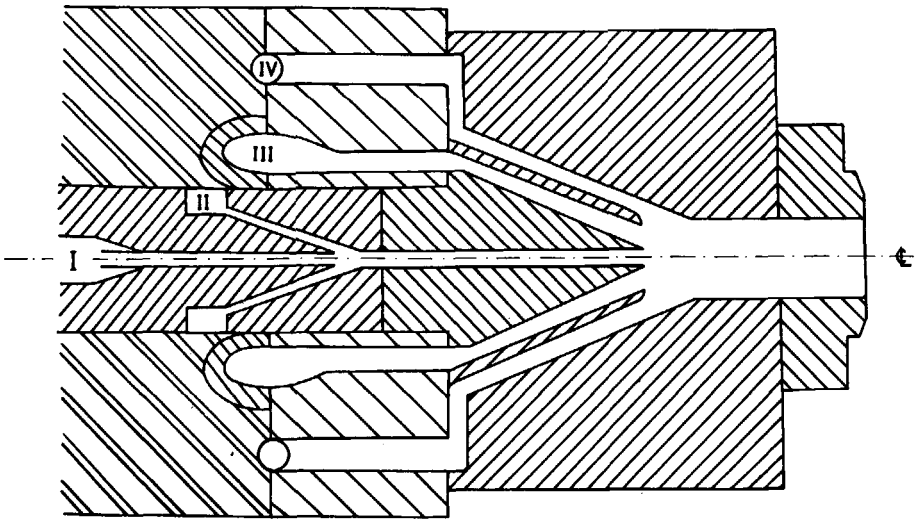

Fig. 1. Schematic representation of multilayered flows through a seven-layer feedlock.

must be found through some numerical method. Quite recently, Mitsoulis[21,22] used the finite element method to solve the full flow equations and showed how to simulate such flows and find the interface and free surfaces of the extrudate iteratively. While the previous work deals exclusively with Newtonian fluids, an extension to power-law fluids is presented here for three typical polymer melts (PS, HDPE, and LDPE) used in a coextrusion experiment by Han.[5] The cases of concentric coextrusion are studied for the same flow rates and melt combinations used in the experimental study. Comparisons are drawn with regard to pressure gradients vs. flow rate between experimental values and numerical results.

MATHEMATICAL MODEL AND MELT PROPERTIES

The steady, creeping, isothermal flow of incompressible, immiscible fluids is governed by the general conservation equations of mass and momentum, respectively:

$$\nabla \cdot \bar{v} = 0 \tag{1}$$

$$0 = -\nabla p + \nabla \cdot \bar{\bar{\tau}} \tag{2}$$

where $\bar{v}$ is the velocity vector, p is the pressure, and $\bar{\bar{\tau}}$ is the extra stress tensor.

A constitutive equation relates $\bar{\bar{\tau}}$ to the rate-of-strain tensor $\bar{\bar{\dot{\gamma}}}$. For a generalized Newtonian fluid assumed in this work,

$$\bar{\bar{\tau}} = \eta \bar{\bar{\dot{\gamma}}} \tag{3}$$

where η is the viscosity given either by a constant μ

$$\text{(Newtonian fluid)} \qquad \eta = \mu \tag{4}$$

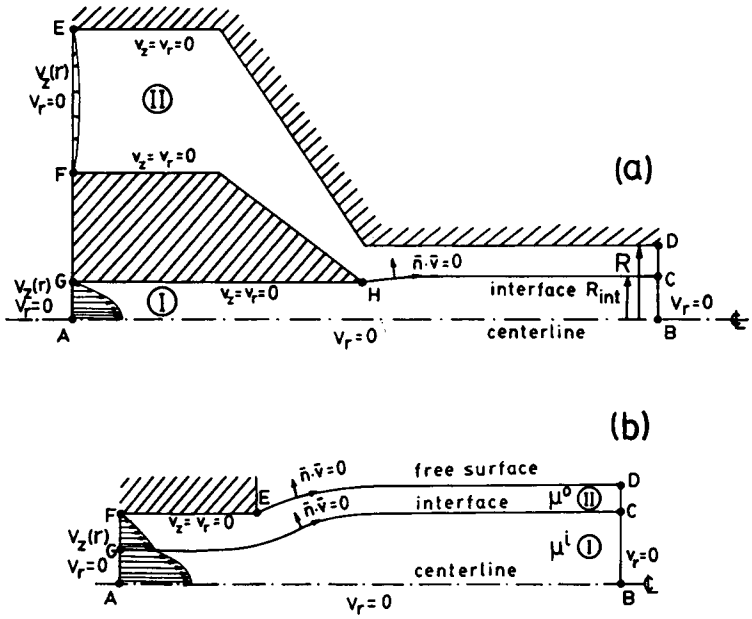

Fig. 2. Velocity boundary conditions and notation for the numerical analysis of a double-layer concentric flow in a feedlock: (a) entry region, (b) exit region.

or by a power-law relationship

$$\text{(power-law fluid)} \qquad \eta = m|\dot{\gamma}|^{n-1} \tag{5}$$

where m is the consistency index, n is the power-law index, and $|\dot{\gamma}|$ is the magnitude of the rate-of-strain tensor $\dot{\bar{\gamma}}$ given by

$$|\dot{\gamma}| = \left[\tfrac{1}{2}\left(\dot{\bar{\gamma}}:\dot{\bar{\gamma}}\right)\right]^{1/2} \tag{6}$$

For concentric coextrusion from capillary dies considered here, the flow domain is axisymmetric and cylindrical coordinates r, z, θ are used.

The solution of the above system of eqs. (1)–(3) is possible after the appropriate boundary conditions have been imposed (see Fig. 2). These consist of no-slip conditions at the solid walls (zero velocities), symmetry at the centerline ($v_r = 0$), fully developed profiles far upstream and $v_r = 0$ far downstream, and zero-surface forces on the extrudate free surfaces. Furthermore, along the interface and the free surface, a no-flow across requirement is used for constructing streamlines.[21] At the interface, continuity of velocities and normal and shear stresses must be satisfied (in the absence of surface tension). This is accomplished by using a finite element method that employs 6-node quadratic triangular elements with continuous pressure variation and *double nodes* at the interface that allow for continuity of velocities but also for discontinuous pressures. More details about the numerical scheme can be found elsewhere.[21,22]

The above analysis can be highly simplified when assuming a fully developed Poiseuille (pressure-driven) flow in a cylindrical tube. The analysis and equations for two power-law fluids flowing in a concentric sheath-core configuration has been given by Han and Chin.[11] Except for Newtonian fluids where an analytical solution exists, the power-law case requires a numerical solution for the system of equations. We have used a full Newton–Raphson iterative scheme to solve the equations and also check the results obtained from the finite element analysis in fully developed tube flow. Knowing the total flow rate Q, the flow rate ratio Q_I/Q_{II}, the tube radius R, and the power-law constants for each melt, the solution gives the interface location λ and the pressure gradient $\zeta = -dp/dz$.

The above mathematical models have been used to simulate the concentric coextrusion experiments for PS, HDPE, and LDPE as given in the paper by Han.[5] The viscosity data have been fitted using least-squares by the following power-law relationships:

$$\text{(PS)} \qquad \tau = 16{,}116\dot{\gamma}^{0.3299} \quad \text{(Pa)} \tag{7}$$

$$\text{(HDPE)} \qquad \tau = 10{,}825\dot{\gamma}^{0.3917} \quad \text{(Pa)} \tag{8}$$

$$\text{(LDPE)} \qquad \tau = 3642\dot{\gamma}^{0.5105} \quad \text{(Pa)} \tag{9}$$

These relations are used both in the fully developed flow analysis and in the finite element analysis for different flow rates and flow rate ratios.

RESULTS AND DISCUSSION

The present simulations have been carried out for the coextrusion experiment performed by Han.[5] Figure 3 shows the die geometry for the case of $L/D = 4$. All lengths have been made dimensionless by dividing by the capillary radius R. The flow entry is extended $4R$ upstream of the contact point H and the final flow exit is extended $4R$ downstream of the die exit point E. Such lengths are necessary to justify the imposition of fully developed profiles as boundary conditions. Due to the long die used, the domain has been split into two regions: entry region: $-4R \le z_{en} \le 4R$, where $z_{en} = 0$ corresponds to the contact point H; exit region: $-4R \le z_{ex} \le 4R$, where $z_{ex} = 0$ corresponds to the exit point E. The results at the outset of the entry region are checked against the fully developed flow results and subsequently used as entry boundary conditions in the exit region.

The finite element grid for each region consists of 520 triangular elements, 1166 nodes (11 points across for each fluid) with a total of 2300 (entry region)/2404 (exit region) nonzero degrees of freedom (unknowns).

Han's experiment with $L/D = 4$, PS forming the inner layer and HDPE forming the outer layer (PS/HDPE), showed that for a total volume flow rate $Q = 89.9$ cm^3/min (1.5 cm^3/s) the interface radius $R_{\text{int},e}$ in the extrudate was about 48% of the extrudate radius R_e. This allows the determination of the flow rate ratio $Q_I/Q_{II} = 0.3$, where I refers to the inner layer (PS). The same procedure has been used for the other cases of melt combinations. Imposing fully developed velocity profiles far upstream corresponding to each individual flow rate, the simulations showed how the interface changed along the die and in the extrudate.

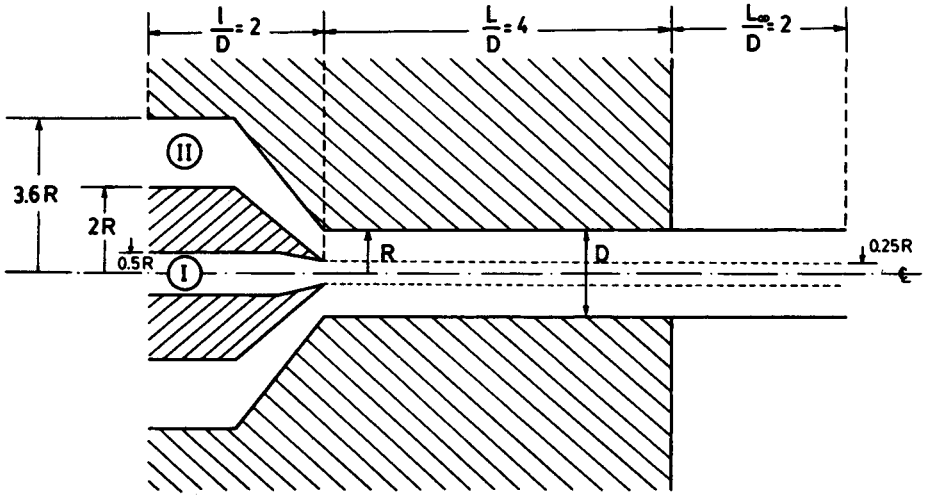

Fig. 3. Coextrusion die design[5] used in the simulation (R = 0.3175 cm, L/D = 4).

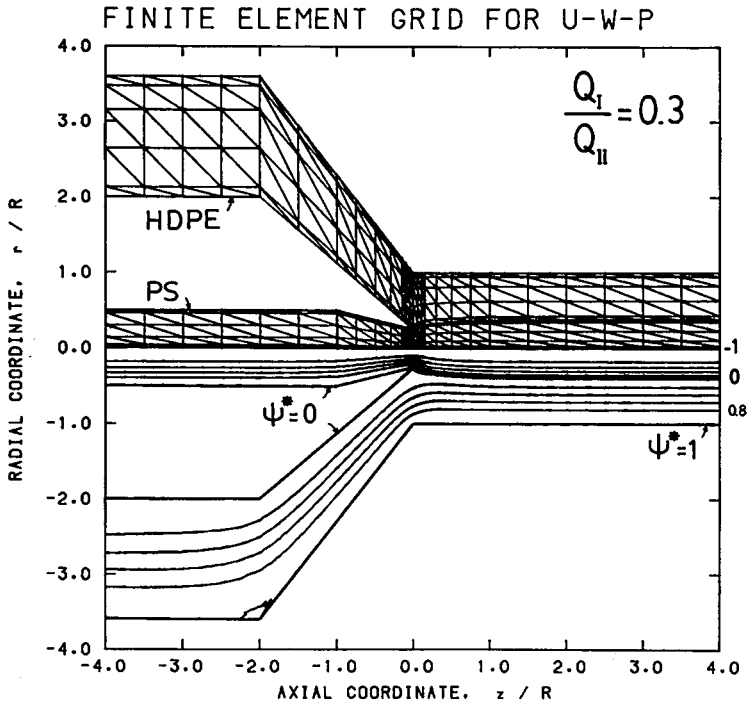

Fig. 4. Numerical analysis in coextrusion of two power-law fluids (Q = 1.5 cm^3/s, Q_I/Q_{II} = 0.3). Entry region: (upper half) final finite element grid; (lower half) streamlines.

Figure 4 presents the final finite element grid (upper half) and the streamlines (lower half) in the entry region for PS/HDPE. The stream function has been obtained *a posteriori* from the solution of the velocity field, and it has been normalized to take the values of -1 at the centerline, 1 at the outer wall and 0 at the inner walls and interface, with increments of 0.2 in between. The corresponding velocity field is shown in Figure 5, where the velocity vectors

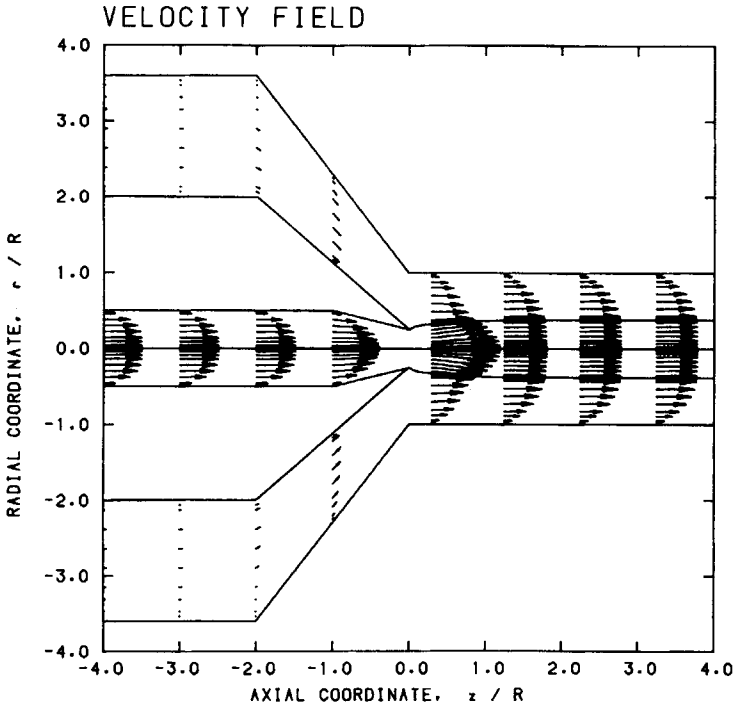

Fig. 5. Velocity field in the entry region (same conditions as in Fig. 4).

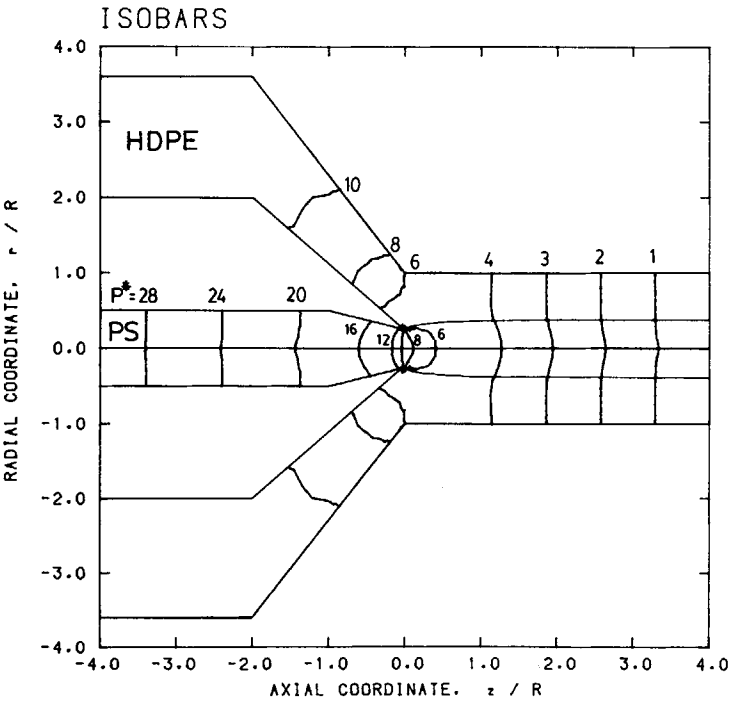

Fig. 6. Isobars in the entry region; $P^* = \Delta P/(\tau_w)_1$ (same conditions as in Fig. 4).

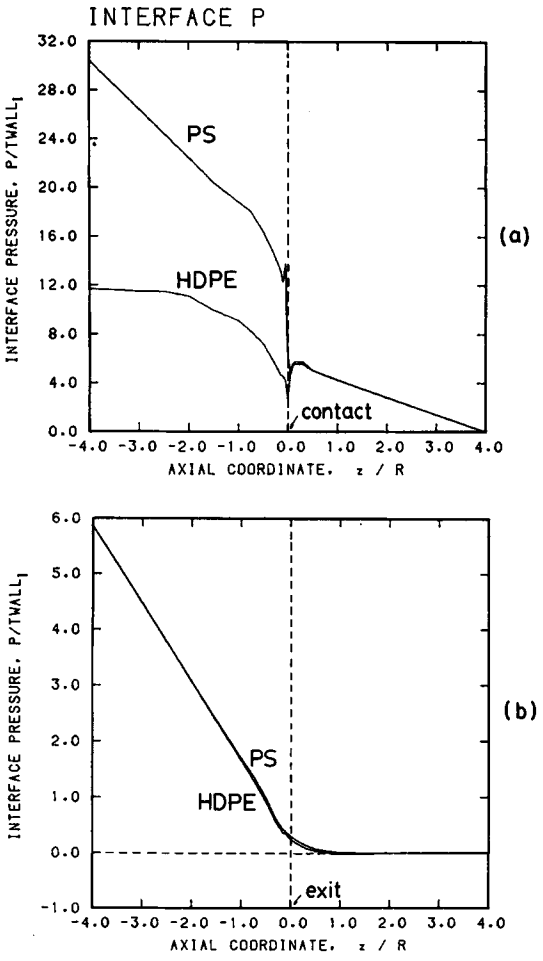

Fig. 7. Axial pressure distribution along the inner walls and the interface: (a) entry region; (b) exit region (same conditions as in Fig. 4).

have been normalized by $\bar{v}_I$, the average entry velocity in the inner tube, and drawn to scale. The pressure results are rendered dimensionless by dividing by the wall shear stress $(\tau_w)_I$ at the upstream entrance of the inner tube. The isobars are shown in Figure 6, where a vertical line corresponds to a fully developed velocity profile (no radial pressure distribution). It was found that a length $L/D = 2$ was sufficient to obtain a fully developed profile at the exit of the entry region. Obviously, this is the case when assuming power-law *inelastic* models. Viscoelastic fluids need a longer distance to fully develop. The axial pressures along the inner walls and on either side of the interface along the flow field are shown in Figure 7. The pressure discontinuities after the contact point are very small, becoming virtually continuous after $0.5R$. The same behavior can be seen near the exit. This is due to the viscosity ratio which is very nearly 1 for these flow conditions ($\dot{\gamma}_w = 83\ s^{-1}$). However, for the case of PS/LDPE, where LDPE is appreciably less viscous than PS, the discontinuities are more pronounced as evidenced in Figure 8.

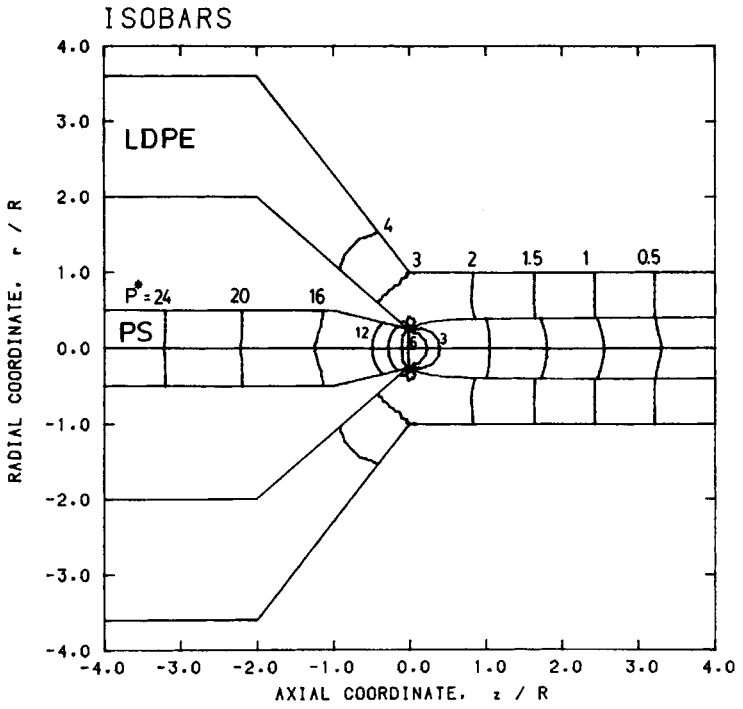

Fig. 8. Isobars in the entry region; $P^* = \Delta P/(\tau_w)_I$ ($Q = 0.893$ cm^3/s, $Q_I/Q_{II} = 0.353$).

With regard to interface location, it was found that the interface changed from its initial value of $R_{int}/R = 0.25$ at contact, to the fully developed value (as found by the simplified analysis) at half way in the die, to $R_{int,e}/R_e$ in the extrudate found from the experimentally obtained pictures. Figure 9 shows the rearrangement of the interface and free surface in the exit region for the PS/HDPE system. It is interesting to note that the finite element results for

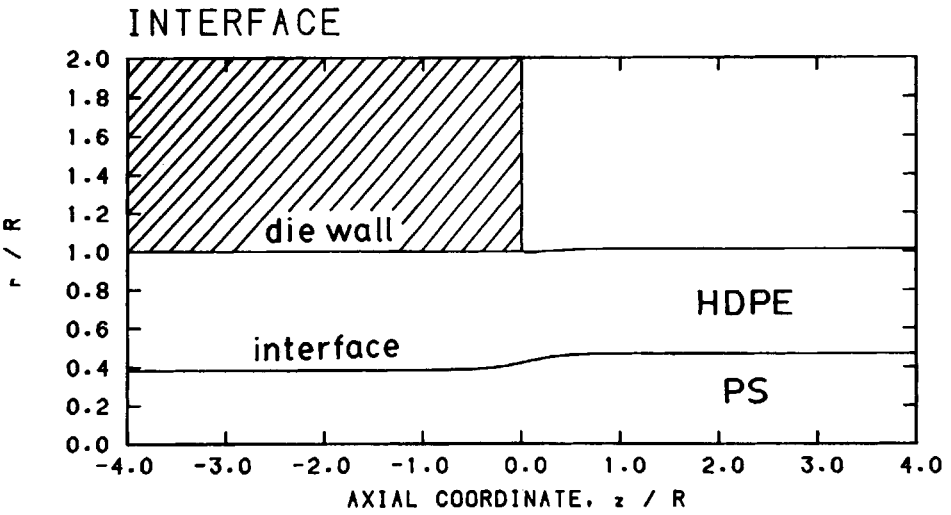

Fig. 9. Interface and free surface in the exit region (same conditions as in Fig. 4).

the interface location agreed within less than 1% with the calculated values from the fully developed flow analysis, but only for the cases of PS (more viscous than HDPE and LDPE) forming the core. For the case of HDPE/PS of comparable viscosities, convergence was very hard to obtain (after 17 interface iterations the error was alternating between $\mp$ 5% of the fully developed value), while for LDPE/PS, divergence occurred. Whether this is an indication of the experimentally observed preference of the less viscous material wanting to emigrate to the walls, is not clear at that point.

The extrudate swell values showed that when the less viscous material (HDPE or LDPE) flows outside the more viscous one (PS), contraction occurs with regard to the swelling of the more viscous component flowing alone. For example, the swell ratio for PS/HDPE was 1.5% and for PS/LDPE was -3.4% compared with 1.6% for PS alone. In contrast, for HDPE/PS the swelling was found to be 2.4%, which is in between the swelling obtained for either component flowing alone (for HDPE, 2.5%). These findings are also in general agreement with previous theoretical[23] and numerical[21] investigations. Since no extrudate swell measurements were made in the experimental study, it is not clear how close the inelastic power-law model can simulate the coextrusion flow of such viscoelastic melts as PS, HDPE, and LDPE outside the die. The extrudate swell values, therefore, should be seen in a relative rather than absolute manner.

The results for the four cases of simulations, shown in Figures 4 and 5 in Han's paper,[5] are summarized in Table I. The overall pressure drops have been obtained by adding the pressure drops of the entry and the exit regions. Since the results obtained for the pressure gradient ($-dp/dz$) were in agreement with the fully developed flow results found from the simplified analysis, no extra finite element runs were made for $L/D = 18$ for which experimental results are given. This is because for inelastic, power-law fluids assumed in this work, fully developed conditions are achieved within a short die length ($L/D = 2$). Thus, a longer die would only influence the overall pressure drop, but not the pressure gradients.

To compare the pressure gradients found experimentally with the results obtained from the fully developed analysis, we have used our Newton–Raphson scheme for the total flow rates given in Figures 8 and 9 in Han's paper.[5] The flow rate ratios were again determined from the photographs given by Han, whenever available. Otherwise, a parametric study was undertaken between the limits of $0 < Q_I/Q_{II} < \infty$.

The results are shown in Figures 10 and 11 for the PS-HDPE and PS-LDPE systems, respectively. It becomes obvious that discrepancies exist even for the case of pure components between experiments and theory. Also the phenomenon of reduced pressure gradient when the more viscous component occupies the core could not be shown by the fully developed analysis of power-law fluids, at least for the range of experimental flow rates. A slight reduction below the value of pure HDPE was found for HDPE/PS but at much higher flow rates ($Q = 13$ cm^3/s, $33 < Q_I/Q_{II} < 1000$, $\dot{\gamma}_w \approx 734$ s^{-1}). Such a possibility has also been shown to exist theoretically by Han and Chin.[11]

The discrepancies evident from the comparisons between theory and experiment may be attributed to several factors. Han[1] and Han and Chin[11] quote viscous heating, slip at the interface between the layers, and slip at the tube wall as some of the reasons. For the present results, the isothermal assump-

TABLE I
Numerical Results from Concentric Coextrusion of Polymer Melts from a Circular Die with $L/D = 4$ ($D = 0.635$ cm)

System	Q^a (cm^3/s)	Q_I/Q_{II}	ΔP (MPa)	$-dp/dz$ (MPa/cm)	$\lambda = R_{int}/R$	$\dot{\gamma}_w$ (s^{-1})	τ_w (MPa)	$R_{int,e}/R_e^a$	R_e/R
PS(I) HDPE (II)	1.500	0.300	3.157 1.525	0.385	0.389	83.1	0.061	0.480	1.015
HDPE (I) PS (II)	1.263	0.333	3.047 1.678	0.422	0.407	75.3	0.067	0.510	1.024
PS (I) LDPE (II)	0.893	0.353	2.299 0.605	0.159	0.407	44.6	0.025	0.510	0.961
LDPE(I) PS(II)	0.465	0.710	— —	0.290	0.468	24.1	0.046	—	—

[a] Experimental data given by Han.[5]

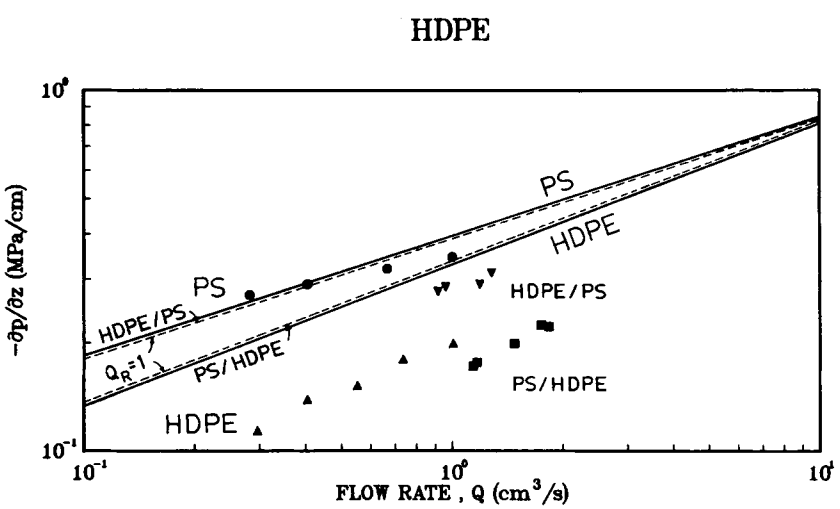

Fig. 10. Pressure gradient vs. volumetric flow rate for the PS–HDPE system: comparison between experiments[5] (symbols) and theoretical predictions (lines) from fully developed flow analysis ($Q_R = Q_I/Q_{II}$).

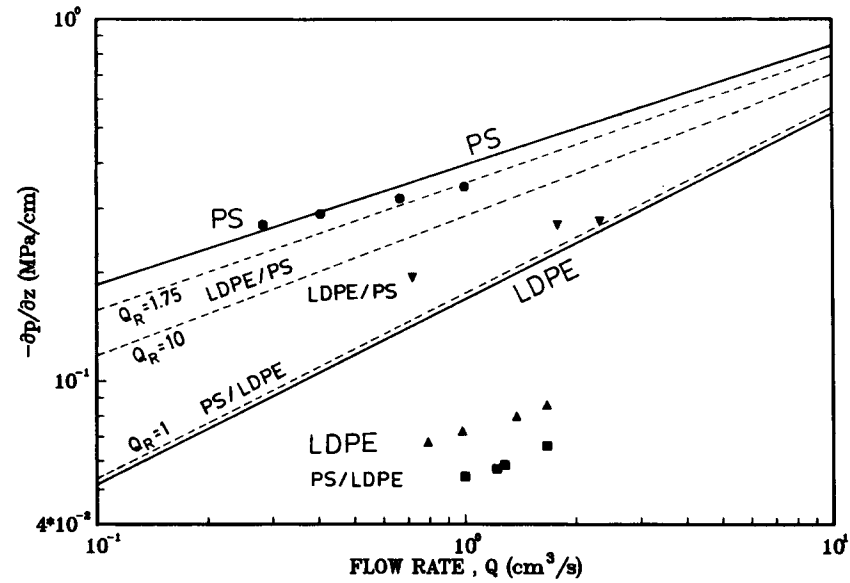

Fig. 11. Pressure gradient vs. volumetric flow rate for the PS–LDPE system: comparison between experiments[5] (symbols) and theoretical predictions (lines) from fully developed flow analysis ($Q_R = Q_I/Q_{II}$).

tion does not seem to be an important factor ($\dot{\gamma} < 100\ s^{-1}$). However, slip at the interface may indeed occur, especially with such incompatible melts as PS and LDPE, as found out experimentally.[11] It also seems that large viscosity ratios are to be avoided, as they may cause interface deformation more easily and sometimes flow instability under certain coextrusion conditions. Finally, the viscoelastic nature of the melts should be taken into account, using an appropriate viscoelastic constitutive equation.

CONCLUSIONS

A numerical simulation of coextrusion flow in a capillary die has been undertaken for polymer melts used in a previously reported experimental study by Han.[5] Experimental viscosity data for PS, HDPE and LDPE melts were fitted by a power law. A Newton–Raphson scheme was employed to solve the equations for a fully developed pressure-driven flow of two concentric layers in a capillary. Also, finite element calculations were performed for the full flow field, before and after point of contact of the two melts up to and after the die exit. The interface and free surface of the extrudate were determined iteratively by constructing streamlines. It was found that for inelastic power-law fluids, a fully developed profile was obtained after a length of 2 tube diameters. The interface ratios agreed closely with experimentally obtained ratios when the more viscous component occupied the core. For the opposite configuration, convergence was very hard to obtain (for the HDPE/PS system) or impossible (for the LDPE/PS system), depending upon the viscosity ratio of the two melts. Swell values showed that contraction occurs when the less viscous material surrounds the more viscous, which is also the preferential configuration in coextrusion. Lack of experimental swell measurements makes it difficult to assess the values found by the present analysis.

Experimental results on pressure gradient vs. volumetric flow rate obtained from long dies ($L/D = 18$) showed discrepancies with the results obtained from the fully developed flow analysis. In particular, the phenomenon of pressure reduction when the less viscous component wets the capillary wall could not be obtained, except for very high flow rates and flow rate ratios. Whether these discrepancies are due to slip at the interface between the layers and/or the viscoelastic nature of the melts is not clear at this point. Further experimental work is needed with well-characterized resins for the shear and elongational viscosity and normal stresses over a wide range of strain rates. Also, extrudate swell measurements in coextrusion are needed to verify the trends found by the finite element analysis.

The finite element method seems quite capable of handling coextrusion flows and determining the interface and free surfaces. A suitable viscoelastic constitutive equation, capable of describing the behavior of polymer melts, should also be implemented to study the effect of viscoelasticity in coextrusion flows. Such an investigation is currently under way by the authors.

Financial assistance from the Natural Sciences and Engineering Research Council of Canada (NSERC) is gratefully acknowledged.

References

1. C. D. Han, *Multiphase Flow in Polymer Processing*, Academic, New York, 1981.
2. J. H. Southern and R. L. Ballman, *Appl. Polym. Sci.*, **20**, 175 (1973).
3. B. L. Lee and J. L. White, *Trans. Soc. Rheol.*, **18**, 467 (1974).
4. N. Minagawa and J. L. White. *Polym. Eng. Sci.*, **15**, 825 (1975).
5. C. D. Han, *J. Appl. Polym. Sci.*, **19**, 1875 (1975).
6. D. L. MacLean, *Trans. Soc. Rheol.*, **17**, 385 (1973).
7. A. E. Everage, Jr., *Trans. Soc. Rheol.*, **17**, 629 (1973).
8. J. L. White and B. L. Lee, *Trans. Soc. Rheol.*, **19**, 457 (1975).
9. A. E. Everage, Jr., *Trans. Soc. Rheol.*, **19**, 509 (1975).
10. C. D. Han and R. Shetty, *Polym. Eng. Sci.*, **16**, 697 (1976).
11. C. D. Han and H. B. Chin, *Polym. Eng. Sci.*, **19**, 1156 (1979).
12. D. D. Joseph, M. Renardy, and Y. Renardy, *J. Fluid Mech.*, **141**, 309 (1984).
13. C. D. Han and R. Shetty, *Polym. Eng. Sci.*, **18**, 180 (1978).
14. Y. J. Kim and C. D. Han, *Polym. Eng. Rev.*, **2**, 239 (1983).
15. C. D. Han, Y. J. Kim, and H. B. Chin, *Polym. Eng. Rev.*, **4**, 177 (1984).
16. G. Sornberger, B. Vergnes, and J. F. Agassant, *Polym. Eng. Sci.*, **26**, 455 (1986).
17. E. Uhland, *Polym. Eng. Sci.*, **17**, 671 (1977).
18. S. Basu, *Polym. Eng. Sci.*, **21**, 1128 (1981).
19. H. B. Chin. Y. J. Kim, and C. D. Han, *Polym. Eng. Rev.*, **4**, 281 (1984).
20. G. Sornberger, B. Vergnes, and J. F. Agassant, *Polym. Eng. Sci.*, **26**, 682 (1986).
21. E. Mitsoulis, *J. Rheol.*, **30**(S), S23 (1986).
22. E. Mitsoulis, *Commun. Appl. Numer. Methods*, **3**, 71 (1987).
23. R. I. Tanner, *J. Non-Newt. Fluid Mech.*, **6**, 289 (1980).

Received November 24, 1986
Accepted February 23, 1987